

# Epitaxial growth and transport properties of $\text{Sr}_2\text{CrWO}_6$ thin films

J. B. Philipp,\* D. Reisinger, M. Schonecke, M. Opel, A. Marx, A. Erb, L. Alff, and R. Gross  
 Walther-Meissner-Institut, Bayerische Akademie der Wissenschaften, Walther-Meissner Str. 8, 85748 Garching, Germany  
 (Dated: received, August 21, 2002)

We report on the preparation and characterization of epitaxial thin films of the double-perovskite  $\text{Sr}_2\text{CrWO}_6$  by Pulsed Laser Deposition (PLD). On substrates with low lattice mismatch like  $\text{SrTiO}_3$ , epitaxial  $\text{Sr}_2\text{CrWO}_6$  films with high crystalline quality can be grown in a molecular layer-by-layer growth mode. Due to the similar ionic radii of Cr and W, these elements show no sublattice order. Nevertheless, the measured Curie temperature is well above 400 K. Due to the reducing growth atmosphere required for double perovskites, the  $\text{SrTiO}_3$  substrate surface undergoes an insulator-metal transition impeding the separation of thin film and substrate electric transport properties.

Double-perovskites of the form  $A_2BB'O_6$  are interesting materials both due to their rich physics and their interesting properties with respect to applications in spin electronics. They are half metallic, i.e. have a high effective spin polarization at the Fermi level [1], and some compounds have a high Curie temperature  $T_C$ , e.g.  $T_C = 635$  K in  $\text{Sr}_2\text{CrReO}_6$  [2]. Large low field magnetoresistance effects are found in  $\text{Sr}_2\text{FeMoO}_6$  [1, 3],  $\text{Sr}_2\text{FeReO}_6$  [4] and  $\text{Sr}_2\text{CrWO}_6$  [5]. Thin films of the well studied system  $\text{Sr}_2\text{FeMoO}_6$  have been fabricated by pulsed-laser deposition (PLD) at relatively high temperatures of about  $900^\circ\text{C}$  [6]. However, epitaxial growth was found to be complicated and difficult to control. There are indications that high structural quality of films grown on  $\text{SrTiO}_3$  is associated with semiconducting behavior [7, 8]. Here, we report on the epitaxial growth of  $\text{Sr}_2\text{CrWO}_6$ . Due to the good lattice match, epitaxial films of this material can be grown on  $\text{SrTiO}_3$  substrates in a molecular layer-by-layer growth mode resulting in high crystalline quality.

$\text{Sr}_2\text{CrWO}_6$  thin films were deposited from stoichiometric targets [5] on atomically flat, HF etched and annealed (001)  $\text{SrTiO}_3$  substrates by PLD using a 248 nm KrF excimer laser [9]. Fig. 1 shows the RHEED (Reflection High Energy Electron Diffraction) [10] intensity oscillations of the (0,0) diffraction spot recorded during the PLD growth of a  $c$ -axis oriented  $\text{Sr}_2\text{CrWO}_6$  film. The molecular layer-by-layer or Frank-van der Merwe growth mode [11] is achieved for a substrate temperature of  $740^\circ\text{C}$ , an argon pressure of  $2 \times 10^{-4}$  Torr, a laser repetition rate of 2 Hz, and a laser energy density on the target of  $1.2 \text{ J/cm}^2$ . RHEED was performed with 15 keV electrons at an incident angle of about  $2^\circ$ . To obtain the number of RHEED oscillations per unit cell, the film thickness has been determined precisely by X-ray reflectometry (Fig. 4) and then divided by the number of observed RHEED oscillations. The derived molecular layer or block thickness corresponds to half a unit cell ( $c/2 = 4.004 \text{ \AA}$ ). Note that the intensity oscillations of the (0,0) and (0,1) spot are out of phase, since for the (0,1) spot the electrons reflected from different growth planes interfere constructively (in-Bragg condition). In this case no RHEED oscillations are expected. The fact that we do observe RHEED oscillations is caused by multiple and diffuse, incoherent scattering which results in an

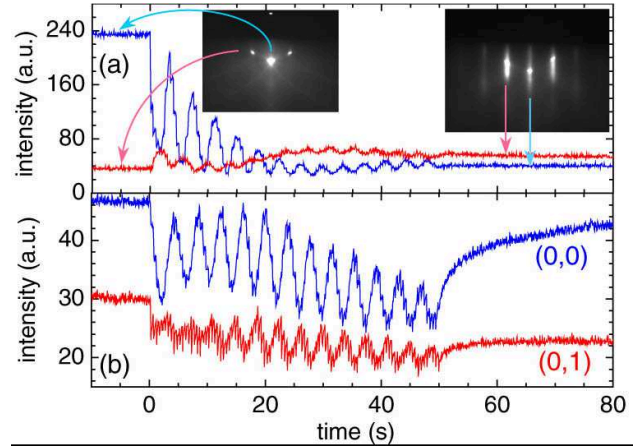


Figure 1: RHEED intensity oscillations observed during the growth of  $\text{Sr}_2\text{CrWO}_6$  on (001)  $\text{SrTiO}_3$  showing a clear  $\pi$ -shift between the (0,0) and (0,1) spot. (a) The first 100 pulses and (b) the second 100 pulses. In (b) the intensity of the (0,1) spot is shifted to lower values for clarity. The inset shows the RHEED patterns before deposition and after 100 pulses as indicated by the arrows.

increasing (decreasing) intensity with increasing (decreasing) step density [12, 13].

Figure 2 shows an *in situ* AFM picture of a 42 nm thick film. Clearly, a terrace structure due to the nonvanishing substrate miscut with about  $4 \text{ \AA}$  high steps corresponding to half a unit cell of  $\text{Sr}_2\text{CrWO}_6$  can be seen. The AFM analysis shows that  $\text{Sr}_2\text{CrWO}_6$  grows as an epitaxial film with a similar crystalline perfection and very smooth surface as the doped manganites [9, 14].

As shown in the inset of Fig. 3, within the resolution of our four circle x-ray diffractometer only (00 $\ell$ ) peaks ( $\ell = 2, 4, 6, \dots$ ) could be detected. Rocking curves of the (004) peak had a full width at half maximum (FWHM) of only  $0.025^\circ$  which is very close to the FWHM of the substrate peak. The fact that Laue oscillations were detected around the film diffraction peaks (Fig. 3) indicates that the strain due to lattice mismatch between film and substrate ( $\simeq 0.1\%$  for  $\text{SrTiO}_3$ ) is not relaxed, i.e. the films grow coherently strained. The unit cell of the high quality strained films has a tetragonal distortion and is slightly larger than the bulk unit cell ( $a_{\text{bulk}} = c_{\text{bulk}} = 7.813 \text{ \AA}$ ,  $a_{\text{film}} = 2 \times a_{\text{SrTiO}_3} = 7.810 \text{ \AA}$  and  $c_{\text{film}} = 8.005 \text{ \AA}$ ). Fig. 4

\*Electronic address: Boris.Philipp@wmi.badw.de

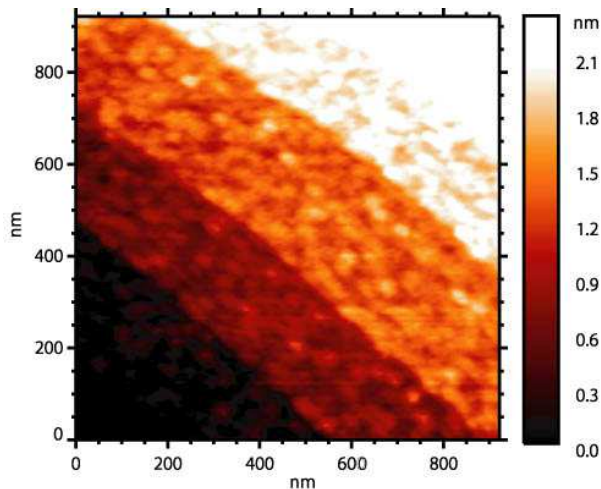


Figure 2: AFM image of a 42 nm thick epitaxial  $\text{Sr}_2\text{CrWO}_6$  film grown on a HF-etched (001)  $\text{SrTiO}_3$  substrate

shows X-ray reflectometry data of a 52 nm thick  $\text{Sr}_2\text{CrWO}_6$  film on a  $\text{SrTiO}_3$  substrate. Fitting the data [15] gives a film thickness that agrees to that obtained from counting the RHEED oscillations to within less than  $\pm 3\%$ . Note that the quality of the fit is extraordinary good.

We have also grown epitaxial  $\text{Sr}_2\text{CrWO}_6$  thin films on other substrates such as  $\text{NdGaO}_3$ ,  $\text{MgAlO}_4$  and  $\text{LaAlO}_3$ . On these substrates a much rougher surface and a more distorted crystal structure is obtained. This is caused by the larger lattice mismatch of these substrates to  $\text{Sr}_2\text{CrWO}_6$  as compared to  $\text{SrTiO}_3$ .

An important parameter of the double perovskites is the sublattice order of the  $B$  and  $B'$  ions (in our case Cr and W). It is evident that for perfect order a superstructure is obtained resulting in a (111) peak in the x-ray diffraction. The intensity of the (111) peak can therefore be used as a quantitative measure of the sublattice order of the  $B$ ,  $B'$  ions. In our  $\text{Sr}_2\text{CrWO}_6$  thin films *no* such peak is found within the experimental resolution for films grown on (001) or (111)  $\text{SrTiO}_3$ , (110)  $\text{NdGaO}_3$ , (001)  $\text{MgAlO}_4$  and (001)  $\text{LaAlO}_3$ . This gives strong evidence that for our epitaxial  $\text{Sr}_2\text{CrWO}_6$  films with high crystalline quality no Cr,W sublattice order is established. It is likely that this is caused by the very similar ionic radii of Cr and W resulting in a very small gain of structural energy by ionic order. We note, however, that despite the complete disorder of the  $B$  and  $B'$  ions a Curie temperature well above 400 K is obtained. This raises questions about theoretical models requiring sublattice order for high  $T_C$ . The saturation magnetization  $M_S$  was found to strongly depend on the growth conditions and the substrate material. A maximum value of  $M_S = 1.9 \mu_B/\text{f.u}$  at 5 K was obtained for a 48 nm thick film grown on (111)  $\text{SrTiO}_3$  at 780°C.

Resistance vs. temperature was measured with a standard four probe configuration. All films not grown on  $\text{SrTiO}_3$  substrates show semiconducting behavior what might be attributed to the large lattice mismatch. We note however, the double perovskite films like  $\text{Sr}_2\text{CrWO}_6$  or  $\text{Sr}_2\text{FeMo}_6$  are grown under very low oxygen partial pressure [6, 8], vacuum

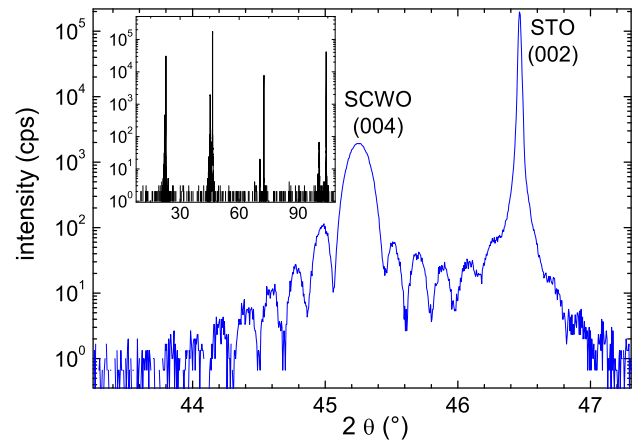


Figure 3:  $\theta$ - $2\theta$  scan showing the (004) peak of a  $\text{Sr}_2\text{CrWO}_6$  film with the Laue oscillations and the (002) peak of the  $\text{SrTiO}_3$  substrate. The inset shows the  $\theta$ - $2\theta$  scan from  $10^\circ$  to  $110^\circ$ .

[7] or Argon atmosphere [5, 8, 16] in a temperature range between 700 and 900°C. Under these conditions (e.g.  $T = 800^\circ\text{C}$ ,  $p_{\text{O}_2} = 1 \times 10^{-8}$  Torr) the surface of the  $\text{SrTiO}_3$  substrates becomes oxygen deficient within a few minutes. That is, a few  $\mu\text{m}$  thick, oxygen deficient surface layer ( $\text{SrTiO}_{3-\delta}$ ) is obtained resulting in a conducting substrate surface [17]. This process is further supported by the reducing plasma during the PLD process. We found that the resistance of the  $\text{SrTiO}_3$  substrate depends strongly on temperature, reducing atmosphere and time. In Fig. 5, the  $R(T)$  curve of a  $\text{SrTiO}_3$  substrate annealed at 820° in Ar is shown as a reference. After the treatment the substrate turns black and shows metallic behavior.

Fig. 5 also shows the  $R(T)$  curve of a  $\text{Sr}_2\text{CrWO}_6$  film grown at a low substrate temperature of only 740°C. Evidently, whether or not the metallic behavior results from the film or the substrate, we have etched trenches into the film (see inset in Fig. 5) interrupting the film and forcing the measurement current to flow in parts through the  $\text{SrTiO}_3$  substrate. As can be seen in Fig. 5 the resistance is still metallic above

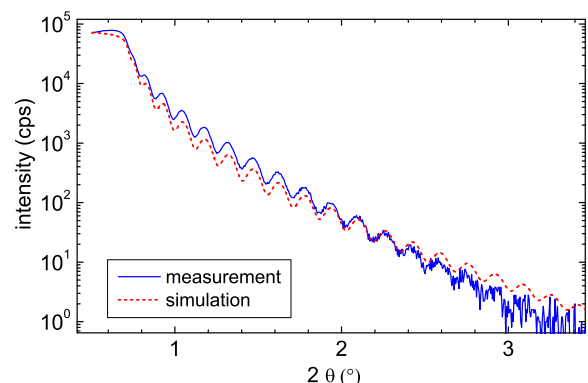


Figure 4: X-ray reflectometry data (solid line) and simulation data (broken line) [15].

50 K but has been increased significantly by roughly one order of magnitude. However, this difference cannot be unambiguously attributed to the interruption of the  $\text{Sr}_2\text{CrWO}_6$  film alone because the trenches are deeper than the film thickness, i.e. the outermost layers of the  $\text{SrTiO}_3$  which may be well conducting are also cut from the current path. Hence, for the  $\text{Sr}_2\text{CrWO}_6$  films on  $\text{SrTiO}_3$  we only have some indication that these films are metallic, however, we cannot definitely prove it at present. Due to the problems of conducting substrate surfaces, in Fig. 5 we plot the resistance of the sample configuration given in the inset and do not plot the resistivity.

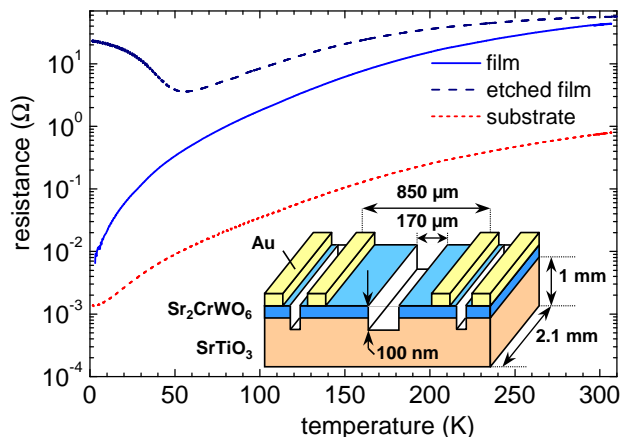


Figure 5: Resistance versus temperature for a 50 nm thick  $\text{Sr}_2\text{CrWO}_6$  film grown at  $740^\circ\text{C}$  (solid line). The inset shows the sample geometry. The dashed line represents the  $R(T)$  curve of the same film after etching a 100 nm deep and  $170\ \mu\text{m}$  wide trench to interrupt the  $\text{Sr}_2\text{CrWO}_6$  film. As a reference, the dotted curve shows the  $R(T)$  curve of a  $\text{SrTiO}_3$  substrate annealed at  $820^\circ\text{C}$  in Ar.

In summary, we have grown epitaxial  $\text{Sr}_2\text{CrWO}_6$  thin films with very high crystalline quality on  $\text{SrTiO}_3$  by PLD. Since the ionic radii of Cr and W are almost identical, no sublattice order of these elements is achieved. Nevertheless, we observe Curie temperatures well above 400 K for these disordered films. The transport properties of the  $\text{Sr}_2\text{CrWO}_6$  films on  $\text{SrTiO}_3$  could not unambiguously be separated from those of the substrate, since the  $\text{SrTiO}_3$  substrate is turned metallic under the reducing deposition conditions.

This work was supported by the Deutsche Forschungsgemeinschaft (project A1/560) and the BMBF (project 13N8279).

- 
- [1] K.-I. Kobayashi, T. Kimura, H. Sawada, K. Terakura, and Y. Tokura, *Nature* **395**, 677 (1998).
- [2] H. Kato, T. Okuda, Y. Okimoto, Y. Tomioka, Y. Takenoya, A. Ohkubo, M. Kawasaki, and Y. Tokura, *Appl. Phys. Lett.* **81**, 328 (2002).
- [3] M. García-Hernández, J. L. Martínez, M. J. Martínez-Lope, M. T. Casais, and J. A. Alonso, *Phys. Rev. Lett.* **86**, 2443 (2001).
- [4] K.-I. Kobayashi, T. Kimura, Y. Tomioka, H. Sawada, K. Terakura, and Y. Tokura, *Phys. Rev. B* **59**, 11159 (1999).
- [5] J. B. Philipp, D. Reisinger, M. Schonecke, A. Marx, A. Erb, L. Alff, and R. Gross, *Appl. Phys. Lett.* **79**, 3654 (2002).
- [6] T. Manako, M. Izumi, Y. Konishi, K.-I. Kobayashi, M. Kawasaki, and Y. Tokura, *Appl. Phys. Lett.* **74**, 2215 (1999).
- [7] H. Asano, S. B. Ogale, J. Garrison, A. Orozco, Y. H. Li, E. Li, V. Smolyaninova, C. Galley, M. Downes, M. Rajeswari, R. Ramesh, and T. Venkatesan, *Appl. Phys. Lett.* **74**, 3696 (1999).
- [8] W. Westerburg, D. Reisinger, and G. Jakob, *Phys. Rev. B* **62**, R767 (2000).
- [9] R. Gross, J. Klein, B. Wiedenhorst, C. Höfener, U. Schoop, J. B. Philipp, M. Schonecke, F. Herbstritt, L. Alff, Yafeng Lu, A. Marx, S. Schymon, S. Thienhaus, and W. Mader, in *Superconducting and Related Oxides: Physics and Nanoengineering IV*, D. Pavuna and I. Bosovic eds., SPIE Conf. Proc. **Vol. 4058** (2000), pp. 278–294.
- [10] J. Klein, C. Höfener, L. Alff, and R. Gross, *Supercond. Sci. Technol.* **12**, 1023 (1999), see also *J. Magn. Magn. Mater.* **211**, 9 (2000).
- [11] T. Terashima, Y. Bando, K. Iijima, K. Yamamoto, K. Hirata, K. Hayashi, K. Kamigaki, and H. Terauchi, *Phys. Rev. Lett.* **65**, 2684 (1990).
- [12] U. Korte and P. A. Maksym, *Phys. Rev. Lett.* **78**, 2381 (1997).
- [13] D. Reisinger, B. Blass, J. Klein, J. B. Philipp, M. Schonecke, A. Erb, L. Alff, and R. Gross, preprint.
- [14] J. Klein, J. B. Philipp, L. Alff, and R. Gross, *phys. stat. sol. (a)* **189**, 617 (2002).
- [15] Bruker AXS Windows RefSim simulation software, based on dynamical scattering theory.
- [16] H. Q. Yin, J.-S. Zhou, J.-P. Zhou, R. Dass, J. T. McDevitt, and J. B. Goodenough, *Appl. Phys. Lett.* **75**, 2812 (1999).
- [17] K. Szot, W. Speier, R. Carius, U. Zastrow, and W. Beyer, *Phys. Rev. Lett.* **88**, 075508 (2002).